

A Platform for Autonomous Navigation in Kiwifruit Orchards

Mark H. Jones^{a,*}, Jamie Bell^{b,**}, Matthew Seabright^a, Alistair Scarfe^c, Mike Duke^a, Bruce MacDonald^b

^a*School of Engineering, University of Waikato, Hamilton, New Zealand*

^b*Faculty of Engineering, University of Auckland, Auckland, New Zealand*

^c*Robotics Plus Ltd, Neunham Innovation Park, Tauranga, New Zealand*

Abstract

This will be written last. General tone of paper is: We present a vehicle designed specifically for autonomous control in kiwifruit orchards. Here are some other people who have made autonomous specific vehicles. Here is ours and this is how it fits in with those. We've gone with these sensors and this method of navigation and it has demonstrated itself to work in the orchard. We think that we could improve the thing by using this algorithm and increasing module space. Generally it is an improvement on the previous work of Scarfe.

Keywords:

Agricultural robotics, outdoor navigation,

1. Introduction

Short-term labor requirements within New Zealand's kiwifruit industry peak twice a year corresponding with pollination and harvesting. The majority of employment during these peaks is filled by seasonal or casual workers (Timmings, 2009). As kiwifruit is the country's largest horticultural export by value (Statistics New Zealand, 2015), automation in this industry may promote economic growth.

Previous work on automated harvesting of kiwifruit has been demonstrated (Scarfe, 2012; Scarfe et al., 2009). That work presents a mobile

*markj@waikato.ac.nz

**jamie977@gmail.com

platform integrated with robotic arms that is capable of harvesting pergola type kiwifruit orchards. The platform presented in this paper is a second generation unit that increases modularity by separating the platform from the tasks it performs. This work discusses only the base platform, where details of modules for harvesting and pollination are published separately (Williams et al., 2017; Seabright et al., 2017).

Automation in kiwifruit harvesting and pollinating demands computer control, state-of-the-art manipulators, and convolutional neural networks. These systems are bulky and have specific geometric requirements dictated the environment and the tasks they perform. They share the requirements of transport to and from orchards, electrical power, and air pressure, but differ in the way they move when in the orchard. The pollinating module moves at a well-known velocity with minimum changes in angle, whereas the harvester advances a set distance between stationary harvest cycles. The duration of a harvesting cycle is determined by the number of fruit to be harvested during that particular cycle. Therefore, as the harvester is designed to be autonomous, there must be communication between the harvester and platform to trigger forward movement between cycles.

It has been stated that “since the robot development already includes a high complexity, the application itself should be of comparably low complexity” (Ruckelshausen et al., 2009). By separating development of the base platform from the task-specific modules, risk of over-complexity is reduced by way of separation. The platform presented here simply needs to transport task specific modules autonomously through kiwifruit orchards.

The development of autonomous vehicles in agriculture is not new, but much of the literature relates to existing vehicles converted to driverless. This paper focuses on the development of a purpose built platform for the purpose of carrying robotic modules through an orchard environment.

2. Review

2.1. Purpose-built Autonomous Vehicles

The introduction of computers and digital camera technology during the 1980s sparked research into creating autonomous vehicles for agricultural use Li et al. (2009). When publishing details of an autonomous vehicle in 1999, Tillett et al. cites difficulties dealing with variability in lighting and the environment as the reason no commercial ready vehicles were available at the time. Their vehicle combined wheel encoders, a compass, and accelerometers



Figure 1: The robot platform driving through a kiwifruit orchard.

for odometry information, and featured a camera based row guidance system. It was capable of spraying individual plants whilst autonomously driving at 2.5 km h^{-1} .

In 2002, two autonomous robots designed for weed mapping and control were published (Pedersen et al., 2002; Åstrand & Baerveldt, 2002). The platforms in these works were relatively simple in terms of their design, referring only to the chassis and drive system, as they are still in a prototype stage. Both were Ackermann based and designed for field crops. The vehicle presented by Pedersen et al. (2002) was designed to follow pre-defined paths through row-crops, but the authors found that this was impractical without a dedicated row guidance sensor. They proposed a revision of their prototype that featured four wheel steering and drive system and integrating both GPS and a row guidance measurements. This work demonstrates a need to combine data from multiple sensor types, which becomes the standard henceforth. Mention at this time was made of utilising a Controller Area Network (CAN) to communicate with drive and steering modules on the revised unit due to it being a dominating standard in agricultural vehicles.

Did this next prototype ever get published?

Bak & Jakobsen (2004) present a relatively advanced robotic platform based on a four wheel steering geometry. The authors noted that the control strategy for the four independently controlled wheels was non-trivial. Like the platform presented earlier by Pederson et al., it combined a compass, gyroscope and GPS for odometry. However, it also featured encoder feedback, a row detection sensor and a GPS unit utilising Real Time Kinematic (RTK) corrections from a base station. RTK-GPS is capable of providing positioning with accuracies of around 2 cm. Their robot utilised a CAN bus for some aspects of system communication.

In 2008, Klose et al. publish details of ‘Weedy’, a autonomous weed control robot for field use. It used a simplistic four wheel steering geometry. There are few details on the sensor selection apart from mention of the use of cameras and ‘acoustic distance sensors’. Presumably the selection of drive geometry on this robot is a cost/complexity optimisation. It too makes use of a CAN bus for communication between on-board modules.

The following year, many the same authors appearing on the ‘Weedy’ paper published details an autonomous robotic platform with four wheel steering named BoniRob (Ruckelshausen et al., 2009). BoniRob had the ability raise and lower itself and alter its wheel placement by actuating the arms to which the motors are attached to. Similar to the unit presented by Bak et al. it features a gyroscope and RTK-GPS for localisation. It introduces the use of both 2D and 3D laser-scanning (or lidar) for perception and row detection. A CAN bus is used to control the low level systems (such as the drive control) and ethernet connections for higher level communication. The authors created a simulated model of the platform using Gazebo in which they could test the many-degrees-of-freedom drive system.

Of particular relevance is the work of Scarfe et al. on an autonomous kiwifruit picking robot (Scarfe et al., 2009; Scarfe, 2012). That work involved the creation of a hydraulically driven platform with Ackermann steering to which four fruit harvesting arms were integrated. While it the ability to navigate a kiwifruit orchard was not tested, it formed the foundation for the second-generation platform presented here.

Blackmore et al. (2007) envisaged significant reductions in production costs by re-purposing parts already in use in the agricultural and automotive industry. While not a physical component, the CAN is one such technology borrowed from the automotive industry aiding developmental of low-level communications. Many of the platforms reviewed, especially the more recent ones, made use of this protocol for real-time communication. Platforms

designed for open field crops appear to favor four-wheel steering over the more traditional Ackermann geometry. The use of simulation tools allowed the creators of BoniRob to develop and test their mobility system separate of the physical hardware.

Common among these vehicles is the use of sensor fusion, whereby data from multiple sensors is merged and filtered. This provides a way to combine the advantages of multiple sensor types, and the benefit of redundancy into a single computation space. With regards to the use of RTK-GPS in perception based guidance systems, Slaughter et al. points out the trade-off of requiring an “unobstructed “view” of the sky from all parts of the field” (Slaughter et al., 2008). Additionally, multi-path signal propagation caused by nearby foliage or the geometry of the land itself presents its own mode of failure (Durrant-Whyte, 2005). This requirement can not be satisfied under the canopy of a kiwifruit orchard which are usually surrounded by tall wind-breaking hedges. A separate feasibility analysis highlighted the use of RTK-GPS systems as a significant cost in yearly subscriptions alone (Pedersen et al., 2006). Torii suggests a combination of both RTK-GPS and machine vision systems to be the most promising system going forward based on reductions in costs and increases in performance of these systems Torii (2000). While Li et al. (2009) concludes that either GPS and machine vision, or GPS and lidar will be used together as a development trend.

2.2. Sensors for Row Based Navigation

Sensors for orchard based row detection fall into two three categories; camera based, lidar based, or a combination. Lidar come in two flavours: single-plane, and multi-plane.

Subramanian et al. (2006) tested both camera based guidance and lidar (Sick LMS-200) based guidance systems in a citrus fruit orchard. Sensors were trialled separately on a tractor retrofitted with a fly-by-wire system. It was able to navigate through the test area at up to 3.1 m s^{-1} using lidar; the authors cite limitations in data acquisition rate from the lidar as the limiting factor. Their vehicle able to navigate at all speeds to an “acceptable” performance level using the machine-vision system, with path errors below 60 mm. They suggest that combining the two systems would give more robust guidance as well as providing the ability to detect obstacles.

Barawid et al. (2007) fit a single-plane lidar (Sick LMS-219) to a tractor for row guidance between tree rows. The authors determine a speed of 0.36 m s^{-1} is appropriate for autonomous navigation on their system as this

produced minimal errors of 0.5° in heading and 50 mm in position. The platform also utilised RTK-GPS receiver and a fibre optic gyro, but only the lidar was used for guidance.

Hansen et al. (2011) use a single-plane lidar (Sick LMS-200) fitted to a drive-by-wire tractor conversion. The vehicle was also fitted with a RTK-GPS receiver, fiber optic gyro. This work focuses on comparing software filters for localisation, rather than path planning.

He et al. (2011) combine camera and GPS receiver on a small electric truck (non-autonomous). They use traditional machine vision algorithms to generate a path between rows of trees in an orchard. The authors note that it may not be suitable when the background becomes complex.

Torres-Sospedra & Nebot (2011) combine neural networks and cameras to generate paths between rows of an orange orchard. Their research focused on the generation of a centre-line rather than full autonomous navigation. The results they obtain from the inclusion of neural networks prove robust in various lighting conditions.

Scarfe (2012) developed a platform designed to be autonomous in kiwifruit orchards. That work combined traditional camera based image processing techniques with a single-plane lidar (Sick LMS-111). The image based approach failed to cope with variability in lighting conditions, however the lidar proved useful for detecting the trunks and posts of the row.

Freitas et al. (2012) angled 2D lidar, encoders, inertial measurement unit. Zhang et al. (2014) Rotated 2D lidar; lidar rotation, wheel and steering encoders Bergerman et al. (2015) Autonomous orchard vehicle Horizontal 2D lidar, wheel and steering encoders. Bargoti et al. (2015) Apple orchard localisation. Vertical 2D lidar, Global Positioning Inertial Navigation System Sharifi & Chen (2015) Orchard row detection Camera.

3. Vehicle design

The canopy of a kiwifruit orchard ranges between 1300 mm and 1700 mm. Modules designed to be carried by the platform require clearance from the canopy, in addition to height they occupy themselves. To maximise space available to these modules the platform must be low-slung at the point of attachment. Figure 2 illustrates the design, with module area allocated between markers ‘F’ and ‘E’ in the side view (top left). The height of the chassis in this region is 360 mm from the ground.

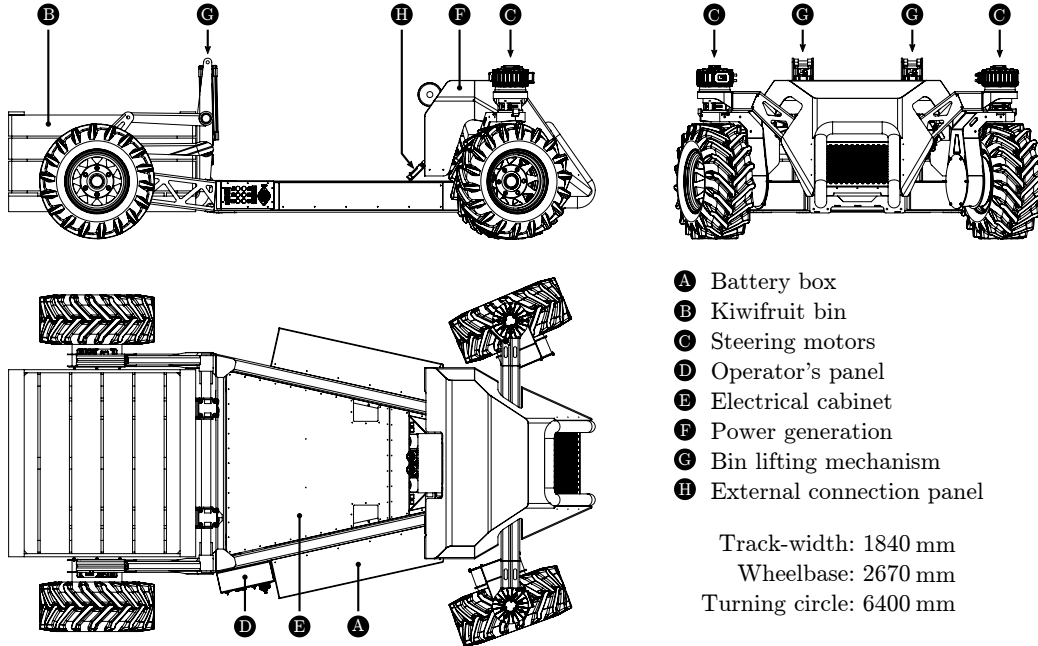


Figure 2: Profile drawings of the robotic platform with kiwifruit bin.

Steering geometry is Ackermann based with independent motors on the front wheels for actuation. The ability to actuate the angles individually simplifies the mechanical geometry needed to coordinate steering, particularly at extreme steering angles. Each steering wheel has the freedom to rotate 340°, limited by a mechanical stop. This range of steering angle allows the vehicle to place the centre of rotation between its rear wheels. At this angle, the turning circle is equal to approximately twice the length of the vehicle. Implementing four wheel steering would allow the centre of rotation to move to the centre of the vehicle, decreasing the turning circle to the total length of the vehicle. However, headlands in kiwifruit orchards are sized for tractors to turn between rows, tractors which use Ackerman steering geometries. The implementation of Ackermann geometry on the platform simplifies the mechanical design, removes the need to develop “non-trivial” control strategies, and increases the usable area. A differential drive, or skid steer, system was expected to cause ground damage to a level considered unacceptable to orchard owners.

Bin lifting forks has been fitted to the area between the rear wheels. This area is sized to accommodate a standard kiwifruit bin. The lifter is

actuated by two vertically mounted pneumatic cylinders and is controlled by a standard pneumatic valve block. This allows the platform to pick-up and drop-off bins as necessary while operating in the orchard; a task expected to be automated in future.

Other than its tires, the platform has no suspension. It features a front pivoting axle that ensures that a minimum of three wheels are always in contact with the ground. Each wheel is mounted directly to a 40:1 fixed ratio planetary gear gearbox connected to a permanent magnet, brushless AC motor. The gearbox-motor combination allows the platform to travel at a maximum speed of 10 km h^{-1} . At this speed in an orchard a full suspension system is unnecessary. In total, the drive system is capable of delivering 25.6 kW of power and 3.3 kN m of torque continuously. With these specifications it is capable of accelerating from a stand-still to its maximum speed at an incline of 20° whilst carrying a 600 kg payload in 2.0 s.

At the front of the platform sits a power generation unit including a petrol engine, air compressor, and alternator. The drive shafts of each are connected by a timing belt. The compressor and alternator are activated electronically by an embedded controller module. Fuel and compressed air tanks sit over the right-hand rear wheel; both are visible in figure 1. Battery modules attached to the sides of the chassis each house fifteen lithium-iron-phosphate batteries.

Unloaded, the machine has an estimated mass of 850 kg, including the power generation unit. It is capable of carrying a 1000 kg payload. The mass of a standard bin of kiwifruit can be as much as 400 kg, leaving 600 kg for modules.

4. Navigation Sensor Selection

4.1. Cost Benefit Analysis of Sensors

The costs of different sensors for a single unit were collated by contacting various manufacturers and suppliers; these results were used to estimate cost ranges for each sensor type. The benefits and issues for each sensor type were noted, based on previous experience and results. All of this information is summarised in Table 4.1.

This data seemed to indicate that the sensors that deliver the most functionality are lidar, cameras and time of flight cameras. In addition, these three sensor types are a reasonable price, at the lower end of their cost range; especially for time of flight cameras, although these sensors have a serious

issue with degradation in performance in sunlight. Because localisation is such a key functionality, GPS also seemed like an important option to test. From this data and since the AMMP has built-in encoders, it seemed to make sense to use encoders to assist with mapping, localisation and velocity feedback.

Table 1: A sample of the sensors considered and parameters used for sensor selection for the AMMP navigation system.

Sensor Type	Manufacturers Considered	Cost Range (USD)	Navigation Applications	Issues
GPS	Ublox, Garmin, Omnistar	50- 4000 per annum	Localisation, pose and velocity measurement	Signal loss under the kiwifruit canopy
IMU	InvenSense, Analog Devices	50- 3000	Acceleration and angular velocity measurement	Thermal drift, accumulated errors
Digital Compass	Honeywell, KVH	50-500	Heading measurement	
Encoders	CUI	30-50	Dead reckoning, velocity measurement	Accumulated errors
2D Lidar	Hokuyo, SICK	2000-10000	Mapping, localisation, pose and velocity measurement, obstacle detection	Tend to not work well in fog and heavier rain
3D Lidar	Velodyne, Quanergy, Neptec	4000-90000	Mapping, localisation, pose and velocity measurement, obstacle detection	Tend to not work well in fog and heavier rain
Time of Flight Cameras	Intel, Basler, Fotonic, Odos Imaging	100-9000	Mapping, localisation, pose and velocity measurement, obstacle detection	Tend to not work well in sunlight conditions, fog and heavier rain
Cameras	FLIR, Basler	500-1500	Mapping, localisation, pose and velocity measurement, obstacle detection	Tend to not work well when visibility is low
Thermal Cameras	FLIR, Optris	3000-14000	Pedestrian detection	In hot conditions, this sensor becomes less useful for pedestrian detection
Radar	Delphi	3000-5000	Object detection	

4.2. Sensor Data Collection and Inspection

The sensors that seemed important to test, based on both the literature survey and the cost-benefit analysis were lidar, cameras and GPS. In addi-

tion, time of flight cameras were considered, because they seemed to be a compelling option based on the cost-benefit analysis; especially if some of the less expensive models were found to work well in sunlight. It was also decided that encoders would be tested in favour of using an IMU because the encoders were built into the AMMP motors. Some data was collected from each sensor in order to decide which sensors to prototype algorithms for.

4.2.1. GPS Data Collection

Two GPS modules were tested. Both were connected via serial to a Beaglebone Black single board computer. The GPS set-ups tested were:

- Ublox Neo-M8N module, selected for its superior navigation sensitivity of -167 dBm and internal Low Noise Amplifier (LNA), additional 20 dB gain/ 0.8 dB noise LNA and active circuitry for the 25mm square ceramic patch antenna.
- OmniSTAR 5120VBS module, with AX0 series antenna, with 34 dB gain/ 1.4 dB noise LNA. The AX0 series antenna claims high multipath rejection.

The procedure used for data collection was:

1. A route through a kiwifruit orchard was planned and plotted on a satellite map. The route was designed to include long stretches underneath the canopy and some areas with a good view of the sky.
2. The distance between post centres along the planned route was measured using a tape measure.
3. The GPS data collection setups were turned on at the starting point of the planned route and were left to initialise for 30 minutes.
4. The data collection unit was carried along the planned route, stopping at each pole. At each pole, the data collection unit was placed near to the pole in an orientation that was repeated for every pole along the route.
5. Step 4 was repeated until the entire route had been traversed and every pole along the way had been (approximately) mapped by the data collection unit.

It was noticed during testing that the signal quality lights on both GPS setups were regularly indicating loss of GPS fix. Although the entire data

collection procedure was performed, many of the results, such as the measurement of spacing between trees and performance, are far less significant than the regular loss of the GPS fix.

The orchard used for the data collection was Batemans at 48 Newnham Road, Whakamarama, New Zealand. A path followed and the corresponding GPS data collected from the different setups is shown in Figure 3. Note that the path followed was traversed twice- once going out and once returning. The data was collected at a slow walking speed- the entire path of approximately 500 metres took in the order of 15 minutes to complete, including stops about every 5.5 metres within the orchard. Multiple sets of data were collected but Figure 3 is indicative of the results.

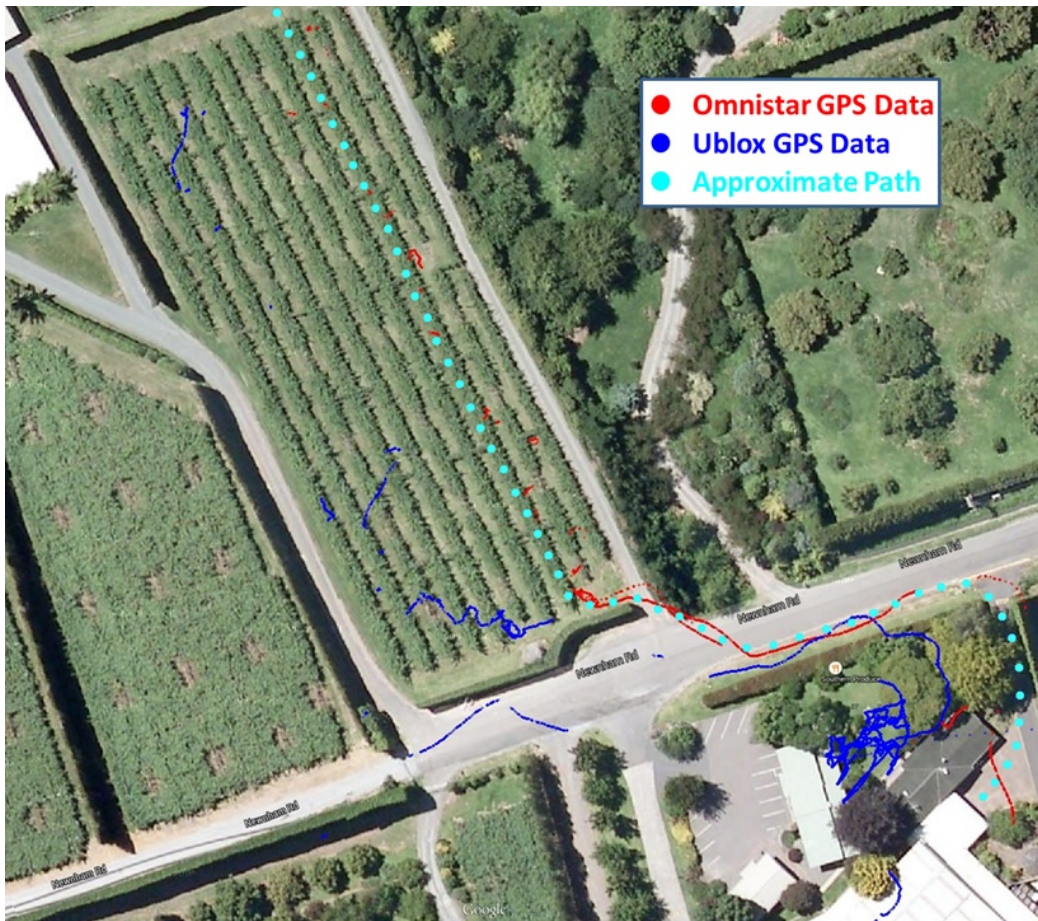


Figure 3: Aerial view of a path through a kiwifruit orchard and the associated GPS data.

The Omnistar GPS setup appears to track the approximate path well but the data is sparse and there appears to be regular loss of signal in the orchard. The Ublox GPS setup collected more data than the Omnistar setup but was much less accurate. The conclusions of this work are that high quality GPS equipment may be useful to provide sanity checks of the approximate location in the orchard. However, it was decided that GPS could not be relied on to provide localisation and other feedback, under the kiwifruit canopy.

4.2.2. Time of Flight Cameras

Two models of Time of Flight cameras were tested. The first was the Basler tof640-20gm-850nm. This sensor provides depth and return signal data at a resolution of 640 pixels wide by 480 pixels high. It was thought that this sensor might work well in sunlight because it had previously been successfully used to collect data from the underside of the kiwifruit canopy in different lighting conditions, with minimal occurrences of the data being washed out. However, it was found that on bright sunny days and in overcast conditions, there was large amounts of data loss, which was deemed unacceptable for important navigation functions such as obstacle detection.

The second time of flight sensor tested was an Intel RealSense R200. The appealing characteristics of this sensor were its low cost and it was advertised as being able to work outdoors. However, in overcast and sunny conditions, there was complete loss of range data.

4.2.3. Lidar Data Collection

Data was collected from two 2D lidar sensors; these were a Hokuyo UTM-30LX and a SICK LMS111. Data was also collected from a 3D lidar sensor, which was a Velodyne VLP-16. The data was collected by driving along rows in kiwifruit orchards with the sensors horizontal and at a height of 0.8 m, which was approximately midway between the ground and the canopy.

The Hokuyo UTM-30LX exhibited some spurious unexplained measurements. The cause of these erroneous measurements was not determined.

It was thought that the lidar sensors would measure the position of structure defining features in the orchard, such as post, trunks and hedges. Detecting such features would then allow the boundaries of the row to be found for row following or these features could be mapped and used for localisation. However, both 2D lidar sensors produced clouds of unstructured data amongst the structured features, as shown in Figure 4. This was caused

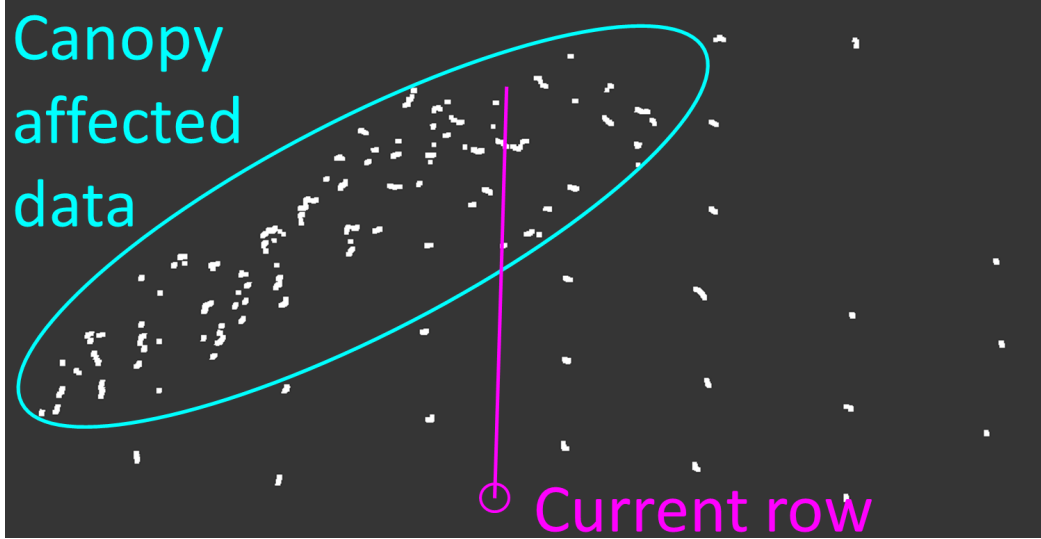


Figure 4: A lidar scan where a region of the data is formed by reflections off the canopy rather than from tree trunks and posts.

by the lidar plane intercepting the canopy on convex slopes and, similarly intercepting the ground on concave slopes (Figure 5) at short ranges.

Data was also collected from the 3D lidar sensor. The 3D lidar sensor had 16 layers of data vertically. As a result on concave slopes, some of the angled up planes had a longer viewing range facing forwards and on convex slopes some of the angled down planes had a longer viewing range facing forwards.

From these results it seemed that the 2D lidar may be a useful sensor at a relatively short range to use for an independent channel of processing for redundancy and increased reliability. However, it was decided to use 3D lidar as a primary navigation sensor because of its ability to be used at longer ranges on undulating ground in kiwifruit orchards.

4.2.4. Camera Data Collection

Data was collected from Logitech C920, Basler Dart daA1600-60uc and Flir CM3-U3-13S2C-CS cameras. Data collection was performed at various times of the day and night, in different weather conditions and different orchards. The data was collected on autonomous and manually driven platforms at a height of approximately 0.8 m from the ground and at speeds of up to 3 ms⁻¹.

It was noticed that the Logitech C920 cameras produced significant mo-

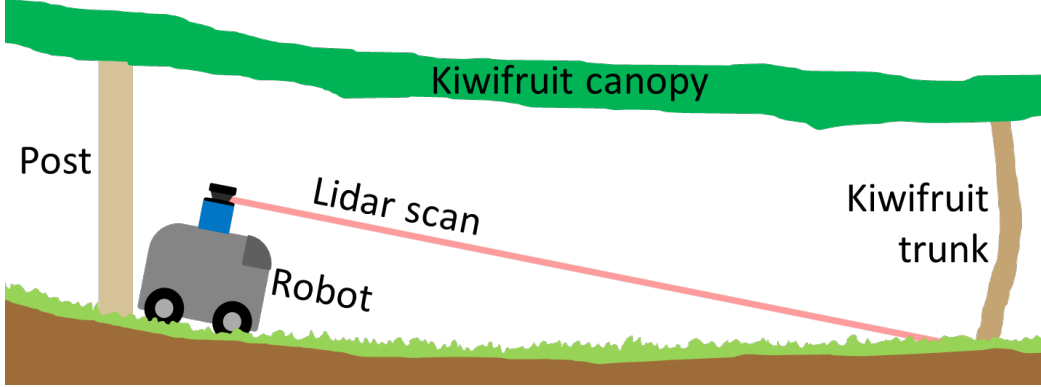


Figure 5: On a concave slope the lidar scan plane may reflect off the ground instead of tree trunks and posts.

tion blur. In addition, these cameras did not provide a hardware trigger interface, which would be important if the cameras were used for stereovision. No image quality issues were noticed with the Basler and Flir sensors; however, the Basler camera was favoured for its later model image sensor.

In terms of sensor selection, the camera images seemed acceptable for performing object detection and classification. This was checked by processing the data using readily accessible algorithms.

4.3. Sensor Demonstration by Prototype Algorithm

The 3D lidar and cameras seemed to be the best of the sensors considered for use as the main sensors for the navigation system. The overall project goals for the navigation system fall into the following categories:

- Object detection and classification.
- Mapping and localisation.
- Driving through the rows of orchards.

In order to validate that the 3D lidar and camera could perform these functions, prototype navigation algorithms were created using these sensors.

4.3.1. Object detection and classification

Object detection and classification was firstly prototyped fully on the camera data. It was decided to use a Convolutional Neural Network (CNN)

for this purpose, because of the existing success of using CNNs for various image processing tasks (LeCun et al., 2015). The CNN architecture chosen was FCN-8s (Long et al., 2015), which is a neural network made up of convolutional layers without fully connected layers, as opposed to having convolutional layers at the input and fully connected layers at the output. FCN-8s performs semantic segmentation, which is the per pixel labelling of images. In order to train the FCN-8s network, the camera image dataset, which was created in order assess the cameras for sensor selection, was reused and hand labelled. The hand labelling consisted of drawing outlines of objects of interest in an image, filling those outlines with colours that were defined to correspond to the given object, extracting the drawn pixels out onto a blank image and converting the result to a palleted indexed format. An example of an original image and a corresponding label image is shown in Figure 6.

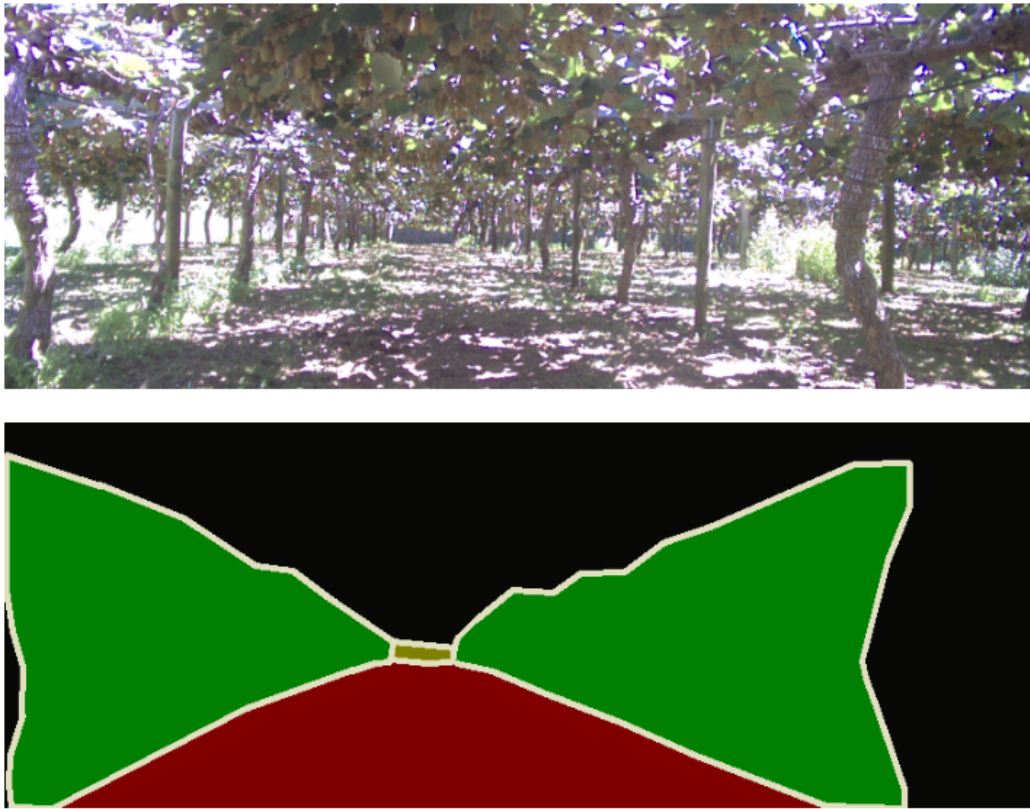


Figure 6: An input image (top) and labelled output (bottom) for semantic segmentation.

Some experimentation was performed with labelling individual trees and posts in the kiwifruit orchard. However, what seemed to work best was to label the entire treeline, consisting of trees and posts as a single class. The list of objects that were labelled during algorithm prototyping were:

- The traversable space, which was defined as the ground in the image that the AMMP could drive a direct path to without collision.
- Treelines.
- The end of the row.

The labelled data was used to train an FCN-8s network. An example of the output from the trained network is shown in Figure 7.



Figure 7: An example result from the FCN-8s network, segmenting a kiwifruit orchard row.

4.3.2. Mapping and Localisation

In order to test the use of 3D lidar for mapping and localisation, an existing Simultaneous Localisation and Mapping (SLAM) package was used. The package used Gmapping (Grisetti et al., 2007), implemented as a ROS package (Gerkey). The required input for Gmapping was odometry data, which was provided by the wheel encoders, and a single plane of lidar data. The 3D lidar provides 16 planes of lidar data so a conversion had to be performed in order to produce a single plane of lidar data for Gmapping. The most simple approach of extracting a single plane out of the 16 planes

from the 3D lidar sensor was not used because it was thought that this would produce the clouds of unstructured data, which was observed with the 2D lidar sensors. Instead, the approach initially used was:

1. The 4 lidar planes that were closest to horizontal were extracted. These planes were selected because they were the planes that generally detected the least amount of ground and canopy.
2. For each angle of the lidar data, the difference in the range measurement between consecutive layers in the 4 lidar planes was calculated.
3. If all of the differences between range measurements from step 2 at a given angle were less than a set threshold, the minimum of the ranges at that angle was extracted.
4. Each extracted minimum range was used to populate a single plane of lidar data at the angle that the range was originally measured at.

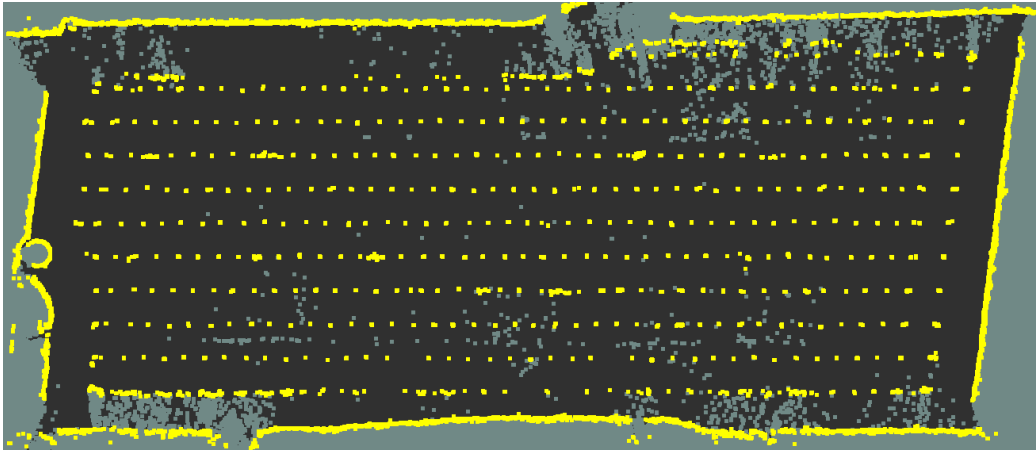


Figure 8: A map of a kiwifruit orchard, created using GMapping, odometry data from encoders and a 3D lidar.

The output of these steps was a single plane of lidar data with reduced amounts of data from the canopy and ground at longer ranges. This data and the encoder data were used as the inputs for Gmapping. By driving along four rows of a kiwifruit block, the map in Figure 8.

4.4. Sensor Selection Conclusions

The results from prototyping algorithms indicate that the 3D lidar and encoder sensors may be feasible selections for performing mapping, localisation and autonomous driving in kiwifruit orchards. Object detection using

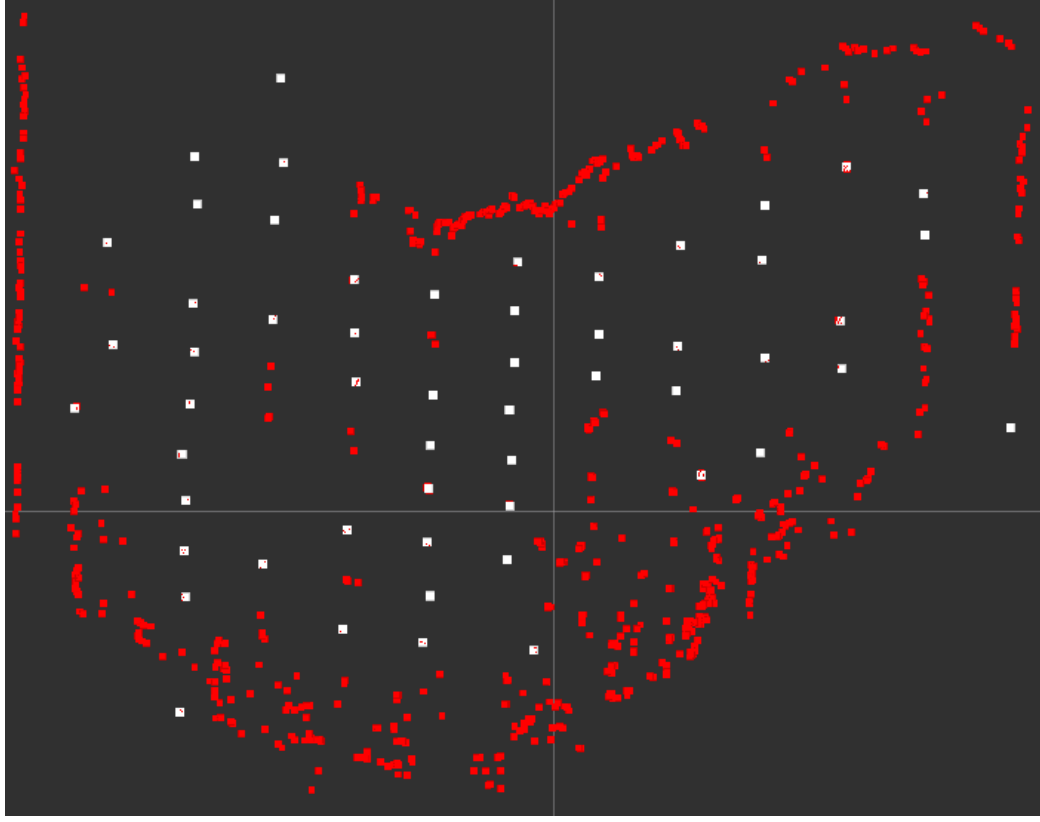


Figure 9: A single plane of the 3D lidar data with the points used for further processing highlighted in white and the rejected points in red.

cameras in kiwifruit orchards also seems possible. Given these results with prototyping algorithms for the navigation system, it was decided to proceed with using cameras, 3D lidar and encoders as the primary sensors for the navigation system.

5. System Architecture

Sub-systems on the platform, including the drive system, are connected to the system PC via a CAN bus, as shown in figure 10. The CANopen protocol has been implemented which offers message type prioritisation and a standardised way of sharing process data. Messages on the bus during operation are restricted to commands, synchronisation messages, and status updates. Relay modules connected to the bus allow the system to control

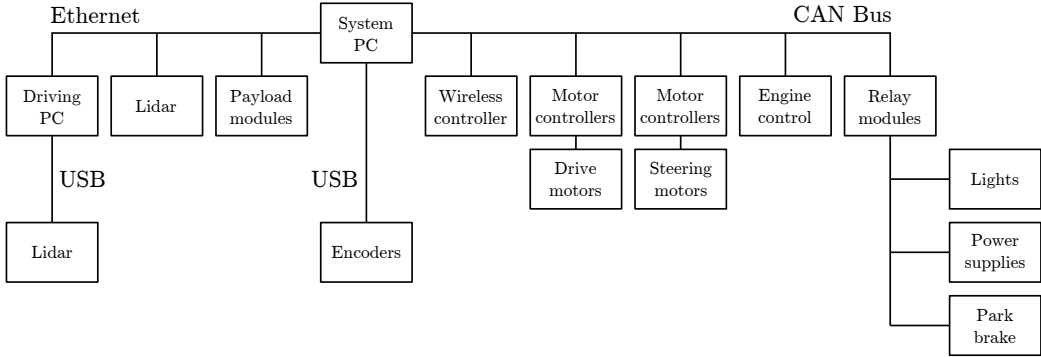


Figure 10: Hardware level system diagram showing the types of interfaces and relative relations on the platform.

the power to its on-board power supplies, motor controllers, park brakes, and lights. They also monitor the timing of synchronisation messages transmitted by the system PC and will enter an error state if the timing falls outside set limits. These messages must be transmitted every 20 ms, with a maximum allowable error of ± 5 ms [check these figures]. Entering an error state results in the motor controllers being disabled, park brakes engaged, and power to the power supplies being cut.

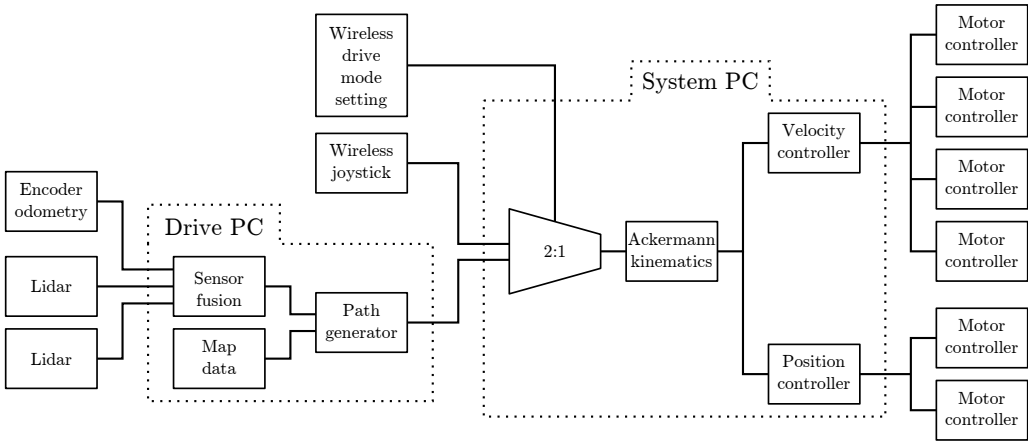


Figure 11: High level system diagram showing software architecture in terms of the manual and autonomous drive system.

A computer dedicated to processing sensing data related to navigation is connected to the platform's "System PC" via Ethernet. The open source

Robotic Operating System (ROS) is used to facilitate communication between the two computers. Not only is ROS used for inter-computer communication, but also within separate software nodes running on the same machine. Figure 11 shows the flow of data from various sources to the motor controllers. For simplicity it omits interface nodes, those used solely to interface the device to the ROS network.

To maximise code reusability, each device on the platform has its own node dedicated to publishing device data or subscribing to generated device commands. Examples of such devices are CAN adapters, motor controllers, wireless controllers, lidar, encoders. Nodes are also used to transform or perform calculations on available data as well as pass it between nodes written in either C++ or Python.

In addition to the drive commands generated by the “Drive PC”, a safety rated wireless controller lets the operator generate commands by joystick. The controller also has a mode selector that selects which commands are fed through to the motor drivers. An emergency stop button on the controller means that the platform can be stopped at any time.

6. Autonomous Driving

It would be great if we could put something in here with regards to how well the platform navigates an orchard. If you don’t want to write it, I can write something generic and put it in for you to approve. Alternatively, you may not want anything in here relating to the navigation performance.

7. Discussion

TODO: Generally summarise the platform, its ability to carry stuff, suitability for the orchard environment, and its ability to drive autonomously.

Acknowledgements

This research was funded in-part by a grant from the New Zealand Ministry of Business Innovation and Employment. The authors acknowledge contributions from Phillip Ross, Gordon Neshausen, Josh Barnett and Erin Simms in the design and fabrication of the platform.



Figure 12: Photo showing the platform performing a row-end turn

8. Jamie-Mark communication

You are free to suggest anything about anything. Maybe you want to add someone to the authors list? Maybe you don't like the focus of the review, or think a review is not necessary. Perhaps you can think of something that would go well in the paper that I've not mentioned.

References

- Åstrand, B., & Baerveldt, A. J. (2002). An agricultural mobile robot with vision-based perception for mechanical weed control. *Autonomous Robots*, 13, 21–35.
- Bak, T., & Jakobsen, H. (2004). Agricultural Robotic Platform with Four Wheel Steering for Weed Detection. *o*, 87, 125–136.
- Barawid, O. C., Mizushima, A., Ishii, K., & Noguchi, N. (2007). Development of an Autonomous Navigation System using a Two-dimensional Laser Scanner in an Orchard Application. *Biosystems Engineering*, 96, 139–149.

- Bargoti, S., Underwood, J. P., Nieto, J. I., & Sukkarieh, S. (2015). A Pipeline for Trunk Detection in Trellis Structured Apple Orchards. *Journal of Field Robotics*, 32, 1075–1094.
- Bergerman, B. M., Maeta, S. M., & Zhang, J. (2015). Robot Farmers. *Robotics & Automation Magazine*, 1.
- Blackmore, B. S., Griepentrog, H. W., Fountas, S., & Gemtos, T. A. (2007). A Specification for an Autonomous Crop Production Mechanization System. *Agricultural Engineering International*, IX, 1–24.
- Durrant-Whyte, H. (2005). Autonomous land vehicles. *Proceedings of the Institution of Mechanical Engineers, Part I: Journal of Systems and Control Engineering*, 219, 77–98.
- Freitas, G., Hamner, B., Bergerman, M., & Singh, S. (2012). A practical obstacle detection system for autonomous orchard vehicles. *IEEE International Conference on Intelligent Robots and Systems*, (pp. 3391–3398).
- Gerkey, B. (). gmapping.
- Grisetti, G., Stachniss, C., & Burgard, W. (2007). Improved Techniques for Grid Mapping With Rao-Blackwellized Particle Filters. *IEEE Transactions on Robotics*, 23, 34–46.
- Hansen, S., Bayramoglu, E., Andersen, J. C., Ravn, O., Andersen, N., & Poulsen, N. K. (2011). Orchard navigation using derivative free Kalman filtering. *Proceedings of the 2011 American Control Conference*, (pp. 4679–4684).
- He, B., Liu, G., Ji, Y., Si, Y., & Gao, R. (2011). Auto recognition of navigation path for harvest robot based on machine vision. *IFIP Advances in Information and Communication Technology*, 344 AICT, 138–148.
- LeCun, Y., Bengio, Y., & Hinton, G. (2015). Deep learning. *Nature*, 521, 436–444.
- Li, M., Imou, K., Wakabayashi, K., & Yokoyama, S. (2009). Review of research on agricultural vehicle autonomous guidance. *International Journal of Agricultural and Biological Engineering*, 2, 1–16.

- Long, J., Shelhamer, E., & Darrell, T. (2015). Fully convolutional networks for semantic segmentation. In *Proceedings of the IEEE Conference on Computer Vision and Pattern Recognition* (pp. 3431–3440).
- Pedersen, S. M., Fountas, S., Have, H., & Blackmore, B. S. (2006). Agricultural robots - System analysis and economic feasibility. *Precision Agriculture*, 7, 295–308.
- Pedersen, T. S., Nielsen, K. M., Andersen, P., & Nielsen, J. D. (2002). Development of an Autonomous Vehicle for Weed and Crop Registration. *International Conference on Agricultural Engineering AgEng2002, Budapest*,.
- Ruckelshausen, A., Biber, P., Dorna, M., Gremmes, H., Klose, R., Linz, A., Rahe, F., Resch, R., Thiel, M., Trautz, D., Weiss, U., Doma, M., & Rahne, R. (2009). BoniRob: an autonomous field robot platform for individual plant phenotyping. *Proceedings of Joint International Agricultural Conference (2009)*, 9, 841–847.
- Scarfe, A. J. (2012). Development of an Autonomous Kiwifruit Harvester, .
- Scarfe, A. J., Flemmer, R. C., Bakker, H. H., & Flemmer, C. L. (2009). Development of an autonomous kiwifruit picking robot. In *Autonomous Robots and Agents, 2009. ICARA 2009. 4th International Conference on* (pp. 380–384). IEEE.
- Seabright, M., Barnett, J., Jones, M. H., Martinsen, P., Schaare, P., Bell, J., Williams, H., Nejati, M., Seok, H. A., Lim, J., Scarfe, A., Duke, M., & MacDonald, B. (2017). Automated Pollination of Kiwifruit Flowers. In *7th Asian-Australasian Conference on Precision Agriculture (7ACPA)*.
- Sharifi, M., & Chen, X. (2015). A novel vision based row guidance approach for navigation of agricultural mobile robots in orchards. *ICARA 2015 - Proceedings of the 2015 6th International Conference on Automation, Robotics and Applications*, (pp. 251–255).
- Slaughter, D. C., Giles, D. K., & Downey, D. (2008). Autonomous robotic weed control systems: A review. *Computers and Electronics in Agriculture*, 61, 63–78.
- Statistics New Zealand (2015). Annual Fruit Exports Hit \$2 Billion for First Time.

- Subramanian, V., Burks, T. F., & Arroyo, A. A. (2006). Development of machine vision and laser radar based autonomous vehicle guidance systems for citrus grove navigation. *Computers and Electronics in Agriculture*, 53, 130–143.
- Timmins, J. (2009). *Seasonal Employment Patterns in the Horticultural Industry*. Technical Report August Statistics New Zealand.
- Torii, T. (2000). Research in autonomous agriculture vehicles in Japan. *Computers and Electronics in Agriculture*, 25, 133–153.
- Torres-Sospedra, J., & Nebot, P. (2011). A New Approach to Visual-Based Sensory System for Navigation into Orange Groves. *Sensors*, 11, 4086–4103.
- Williams, H., Jones, M. H., Nejati, M., Bell, J., Penhall, N., Seok, H. A., Lim, J., MacDonald, B., Seabright, M., Barnett, J., Duke, M., & Scarfe, A. (2017). Robotic Kiwifruit Harvesting using Machine Vision, Convolutional Neural Networks, and Robotic Arms. *Biosystems Engineering*, (p. To be published).
- Zhang, J., Maeta, S., Bergerman, M., & Singh, S. (2014). Mapping Orchards for Autonomous Navigation. *ASABE Annual International Meeting*, 7004, 1–9.